HHS Public Access

Author manuscript

J Ultrasound Med. Author manuscript; available in PMC 2024 December 01.

Published in final edited form as:

J Ultrasound Med. 2023 December ; 42(12): 2815–2824. doi:10.1002/jum.16320.

Correlation of Ocular Plane-Wave Doppler with Optical Coherence Tomography Angiography in Preeclampsia

Ronald H. Silverman, Ph.D.[1], **Raksha Urs, Ph.D.**[1], **Ronald J. Wapner, M.D.**[2], **Ives A. Valenzuela, M.D.**[1], **Hanna R. Coleman, M.D.**[1], **Srilaxmi Bearelly, M.D.**[1]

[1]Department of Ophthalmology, Columbia University Irving Medical Center

[2]Department of Obstetrics and Gynecology, Columbia University Irving Medical Center

Abstract

Objectives: Preeclampsia (PE) is a severe complication of pregnancy characterized by hypertension, proteinuria and compromised fetal blood supply. The eye, like other end organs, is affected by this systemic condition, but unlike in other organs, ocular media transparency allows high-resolution optical visualization of the vascular structure of the retina. Our aim was to assess how ultrasound-determined ocular blood-flow correlates with vascular structure of the retina and choriocapillaris determined by optical coherence tomography angiography (OCTA).

Methods: Plane-wave ultrasound and OCTA were performed on both eyes of 40 consecutive subjects with normal controls (n=11), mild PE (n=5), severe PE (n=17) and chronic or gestational hypertension (n=7) within 72 hours following delivery. From ultrasound, we measured pulsatile flow velocity and resistance indices in the central retinal artery and vein, the short posterior ciliary arteries and choroid. From OCTA, we measured vascular density (VD) in the superficial, deep retina and choriocapillaris. We determined differences in Doppler and OCTA parameters among groups and correlations between ultrasound and OCTA.

Results: In severe PE, flow resistance was reduced with respect to controls. Flow velocity and resistance in the CRA and SPCA were moderately correlated with VD in the choriocapillaris and peripapillary retina, but VD in PE did not differ significantly from controls.

Conclusions: Although OCTA parameters were moderately correlated with Doppler ultrasound, OCTA did not demonstrate significant differences between PE and controls post-partum.

Keywords

Blood flow; Plane-wave Doppler; Eye; Optical coherence tomography angiography; Preeclampsia; Ultrasound

Author of correspondence: Ronald H. Silverman, PhD, Department of Ophthalmology, Columbia University Irving Medical Center, 635 West 165th St., Research Annex Room 711, New York, NY 10032, Phone: 212 305 5484, Fax: 646 426 0202, rs3072@cumc.columbia.edu.

Conflict of Interest: None, for all authors

Introduction

Preeclampsia (PE) is a multisystem disorder usually occurring after 20 weeks of gestation. It affects 4–7% of pregnant women and is implicated in major maternal co-morbidities and adverse perinatal outcomes. PE is characterized by acute onset of hypertension, proteinuria, edema and reduced organ perfusion secondary to vasospasm and activation of the coagulation cascade.[1] Despite extensive research, the cause of PE remains elusive.[2] In the United States, PE accounts for approximately 16% of all maternal deaths and risk of fetal death is highly elevated, especially for PE occurring in the preterm period.[3,4] Women suffering PE are also at risk later in life for high blood pressure, stroke, vascular dementia, heart and renal disease.[5]

While the placenta might be regarded as the most intuitive target for vascular imaging for assessment of PE risk[6], it is far less accessible to high-resolution imaging of the vasculature than is the eye, where the retinal microvasculature can be visualized optically at high resolution. This is especially true given recent advances in ocular imaging, such as optical coherence tomography (OCT) and OCT-angiography (OCTA).

The eye is also more accessible to high-frequency ultrasound than is the placenta. We recently reported increased diastolic flow velocities and reduced resistance indices in the eye in severe PE subjects compared to normal post-partum control subjects examined with plane-wave ultrasound (PWU) within 72 hours of delivery.[7] In this report, we describe association of OCTA parameters with PE and correlation of OCTA and PWU Doppler on forty subjects examined with both techniques.

Material and Methods

This research followed the tenets of the Declaration of Helsinki and was approved by the Columbia institutional review board. Informed consent was obtained after explanation of the nature and possible consequences of the study.

Post-partum human subjects were classified by one investigator (RW) as previously described[8] into one of four groups: normal controls (n=11), mild PE (mPE) (n=5), severe PE (sPE) (n=17) and chronic or gestational hypertension (HTN) (n=7). In brief, patients with systolic blood pressure (PB) >140 mmHg or diastolic BP >90 mmHg were classified as HTN if proteinuria, thrombocytopenia and elevated platelet count were absent, and as mPE if one or more of these were present. Patients with systolic BP >160 mmHg or diastolic BP >110 mmHg plus proteinuria, thrombocytopenia or elevated platelet count with other symptoms including but not limited to severe headache, cerebral or visual disturbances were classified as sPE. Classifications were masked to investigators until ultrasound and OCTA data analyses were complete.

Blood pressure (BP) was measured in the patient’s room prior to and following the ultrasound and OCT exams. Systolic and diastolic BP, pulse rate in beats per minute (BPM) were recorded. Mean arterial pressure (MAP) was calculated as (2*diastolic + systolic)/3. Pulse pressure (PP) was calculated as systolic - diastolic.

Imaging was performed within 72 hours of delivery. Ultrasound exams were performed on both eyes of all subjects by a single investigator (RHS) using a Verasonics (Kirkland, WA) Vantage-128 research ultrasound engine with a Verasonics L22–14vXLF 18 MHz linear array probe having a 12.8 mm aperture. Resolution is approximately 80 μm axially by 250 μm laterally. In the PWU technique, all 128 transducer elements transmit together, instead of the conventional transmission and scanning focused beams. This allows a major increase in imaging speed (up to 18,000 B-scans/sec) and reduced acoustic intensity. The mechanical index (MI) under the transducer excitation conditions used during the exam was 0.07, well under the FDA ophthalmic limit of 0.23.

Ultrasound scanning was performed and data processed as previously described.[7] In brief, scans were acquired in duplicate through the closed eyelid in a horizontal plane. Scan data were acquired for 2.7 sec, allowing acquisition of approximately three cardiac cycles. Scans of the peripapillary region were acquired from two transmit angles (+ and −9°), with compound data acquired at 6,000 images/sec. Scans of the choroid were acquired in a plane superior to the optic nerve, at 1,000 images/sec, each image compounded from 10 angled transmits. Examination of both eyes took approximately 15 minutes.

Analysis of digitized ultrasound data was performed subsequent to the exam. Color flow images were derived from the singular value decomposition filtered data and spectrograms depicting flow velocity at selected locations produced, from which peak systolic velocity (PSV), end diastolic velocity (EDV), mean velocity (MV) and resistive index, RI = (PSV – EDV)/PSV and pulsatility index, PI=(PSV – EDV)/MV, were determined. Figure 1 provides examples of color flow images and analysis.

OCTA data were acquired by an experienced medical photographer on both eyes in a non-mydriatic exam within a few minutes of the ultrasound exam using a Zeiss Plex Elite 9000 swept source OCT (Carl Zeiss Meditec, Dublin, CA). OCTA is based on detection of areas of signal decorrelation between sequential OCT B-scans of the same plane to construct an *en face* map of blood flow.[9]

The instrument's center wavelength is ~1050 nm. The instrument acquired 100,000 vectors per second. Axial and lateral resolutions are ~6 μm and ~14 μm, respectively. 6×6 mm and 3×3 mm images centered on the fovea and optic nerve were acquired. All OCTA data had signal strength of 9 or 10/10. Figure 2 is an example of an OCT B-scan with flow detection.

OCTA slabs (flattened *en face* images) depicting the superficial and deep retina and the choriocapillaris were analyzed. Layer boundaries were automatically determined by the Plex Elite Review software. The superficial retina was defined as encompassing from the internal limiting membrane to the posterior margin of internal plexiform layer. Deep retina is defined as extending from the posterior margin of internal plexiform layer to the posterior margin of outer plexiform layer. The choriocapillaris is defined as the 20 μm layer beneath the retinal pigment epithelium.

Measurements of the area of the foveal avascular zone (FAZ), vascular density (VD) and flow area (FA) of each layer were determined using custom software in Fiji[10] and MATLAB

(MathWorks, Natick, MA). 3×3-mm perifoveal slabs were used for measurement of VD and FA of the choriocapillaris, deep and superficial retina.

FAZ area was determined by applying Li thresholding[11] followed by a series of erosion and dilation operations. The pixel count of the FAZ was then scaled appropriately in mm^2.

VD was determined by thresholding OCTA slabs with an Otsu filter[12] and calculating above-threshold/total pixels after excluding the fovea and optic nerve head regions. FA was determined by counting the above-threshold pixels in Otsu-filtered images of each layer within a 2 mm diameter circle centered on the fovea expressed as area in mm^2 units. FA is thus a special case of VD limited to the immediate surround of the macula. Figure 3 illustrates these processing steps.

Several additional OCT parameters were assessed jointly by investigators HRC and IAV. These included retinal and choroidal thickness measured at the fovea, nasally, temporally, superiorly and inferiorly, arterial and venous tortuosity and presence/absence of ONH edema, FAZ erosion, ‘mothy’ FAZ appearance, and presence of enlarged lacunae and bright spots.

Statistical analysis was performed with IBM SPSS, Version 25 (IBM Corp, Armonk, NY). Means and standard deviations of systemic BP parameters, ultrasound-determined flow parameters, retinal thickness, FAZ area, FA and VD of each layer were determined for each group. Correlation coefficients between ultrasound and OCTA parameters were determined. Mean values of parameters for each group were compared using a General Linear Model (GLM), treating measurements from paired left and right eyes as repeated measures to allow compensation for correlation between eyes. A Dunnett’s post-hoc test was used to assess the significance of differences of means with respect to the control group.

Results

Table 1 shows BP parameters by group. As would be expected, BP was higher in mPE, sPE and HTN than in controls. Pulse rate was elevated only in sPE.

ANOVA of subject age in years (controls: 30.8±7.0; mPE: 34.1±6.9; sPE: 32.5±5.4; HTN: 30.5±9.0) showed no significant variation between groups.

Correlations between systemic blood pressure parameters and ocular flow were in general not significant, with the exception of choroidal EDV with systemic pulse pressure ($R=.321$, $p<.05$).

Neither retinal nor choroidal thickness showed significant differences among groups. We found no significant correlation between retinal or choroidal thickness and VD or FA. No significant differences in FAZ area were found between groups. No significant differences between controls and sPE were found for tortuosity and ONH edema, FAZ erosion, FAZ appearance, enlarged lacunae or presence of bright spots.

Mean PWU Doppler flow parameters for each vessel by group are summarized in Table 3. Resistance indices were lower in all vessels in sPE compared to controls and statistically significant in the choroid.

Neither VD nor FA showed a significant difference with respect to controls in any layer.

Correlation coefficients between PWU Doppler and VD are provided in Table 4 and with FA in Table 5.

For VD, correlations were between peripapillary retinal VD and resistance in the SPCA (R=.380, p=.001). Superficial retinal VD was significantly correlated with choroidal resistance. Choriocapillaris VD and FA were both significantly correlated with flow velocity in the CRA and SPCAs.

Discussion

In this study, we measured ocular blood flow velocity and resistance (functional) using PWU, and vascular density and flow area (structural), using OCTA in a cohort of early post-partum subjects. We compared values of Doppler and OCTA parameters between controls and PE and assessed correlation of blood-flow velocity parameters with VD and FA.

Although both ultrasound and OCTA detect blood flow, they are distinctly different: PWU Doppler provides measurement of flow velocities (in mm/sec) in the choroid and orbital vessels (the CRA, SPCA and CRV) supplying and draining the retina and choroid. Choroidal flow velocities are believed to originate in the larger vessels of Sattler's and Haller's layers rather than the choriocapillaris.[13] Because PWU allows acquisition of thousands of B-scans/sec, pulsatile waveforms are captured allowing measurement of systolic and diastolic velocity and resistance indices. While Doppler analysis allows measurement of flow velocity, volumetric flow is not determined as lumen diameters are unknown. Ultrasound penetration at 18 MHz is ~1 cm.

OCT has over an order of magnitude higher resolution than ultrasound and high-speed scanning allows capture of 3D data and *en face* presentation. OCT is advantageous with respect to ultrasound in being non-contact and requiring less expertise in conducting the exam. Unlike PWU, OCT is available in turn-key commercial instruments. By detecting positions of decorrelation between successive rapidly acquired images, OCTA identifies regions where flow is present. OCTA depicts the presence or absence of flow in the area of interest but does not offer information on flow velocity or direction. OCT penetration is ~1 mm.

While ultrasound Doppler interrogates large caliber vessels supplying the eye, OCTA characterizes the fine capillary network of the retina. Ultrasound and OCTA thus provide distinct but complementary information regarding ocular blood flow and tissue perfusion.

Our observation of decreased vascular resistance in PE is consistent with most prior studies of cerebral, orbital, and retinal blood flow.[14–22]

Our findings agree with those reported by Urfalıoglu et. al. who found no significant difference in VD in the superficial or deep retina in pregnant PE versus control subjects.[23] Urfalıoglu did, however, report reduced FA with respect to pregnant controls in the choriocapillaris, which we did not find. This difference might be attributed to instrumentation or analysis, as different instruments and analysis programs were used. A more likely factor, however, is that their study was performed during pregnancy and ours performed post-partum: Although the pathogenic mechanism of PE is still subject to debate, and possibly multifactorial, the placental origin of PE is widely accepted.[24] Delivery of the placenta is thus the 'cure' for the condition. While subfoveal choroidal thickness has been reported to be increased in PE during pregnancy[25,26], a recent report[27] found no significant difference in the early post-partum period. This together with our own observations and Urfalıoglu's report suggest that the choroid and choriocapillaris blood flow return to normal rapidly following delivery of the placenta.

Vasospasm has long been considered characteristic of PE. In the case of the eye, this is supported by reports of the narrowing of the retinal vessels in PE.[28,29] This, however, is seemingly in contradiction to the reduced resistance reported here and elsewhere. We previously hypothesized that overperfusion of the orbital vasculature might cause the vessels of the choriocapillaris to become congested, resulting in retinal arteriolar vasospasm as a retinal defensive mechanism.[7] What the effect of this would be on OCTA is not obvious, since OCTA detects blood-flow area, but not volumetric flow. Conversely, although ultrasound detects velocity, it does not allow assessment of volumetric perfusion and is unable to assess the choriocapillaris in any case.

Although our findings do not reveal alteration of VD or FD in the choriocapillaris in sPE post-partum, correlations between PWU Doppler flow velocity and resistance with OCTA VD and FA suggest a subtle relationship with OCTA-determined parameters that might be more evident during pregnancy than post-partum.

Conclusion:

In this study, we compared differences between early post-partum PE versus controls using PWU Doppler-determined ocular blood flow velocity and OCTA-determined vascular density, and assessed correlation between the two techniques. We confirmed earlier findings demonstrating significantly reduced arterial flow resistance in sPE and demonstrated moderate correlations between PWU-determined flow velocity and OCTA-determined VD.

Although OCTA cannot at present measure flow dynamics, it allows demonstration of subtle structural changes in the retina[30] and choriocapillaris[23]. While a recent report[23] found significant differences in OCTA-determined FA during pregnancy, this was not the case in the present early post-partum study. The attribution of this to instrumentation, processing methods or timing (pre- versus post-delivery) will need to be addressed in future studies.

Acknowledgements

This work was supported by the National Institutes of Health grants R01 EY025215, P30 EY019007 and National Center for Advancing Translational Sciences grant UL1TR001873, the New York Community Trust – Theresa Dow Wallace Fund and an unrestricted grant to Columbia Dept. of Ophthalmology from Research to Prevent Blindness.

References

1. Ananth CV, Keyes KM, Wapner RJ. Pre-eclampsia rates in the United States, 1980–2010: age-period-cohort analysis. Bmj. 2013;347:f6564. [PubMed: 24201165]
2. Ness RB, Sibai BM. Shared and disparate components of the pathophysiologies of fetal growth restriction and preeclampsia. Am J Obstet Gynecol. 2006;195(1):40–49. [PubMed: 16813742]
3. Harmon QE, Huang L, Umbach DM, et al. Risk of fetal death with preeclampsia. Obstet Gynecol. 2015;125(3):628–635. [PubMed: 25730226]
4. Shih T, Peneva D, Xu X, et al. The Rising Burden of Preeclampsia in the United States Impacts Both Maternal and Child Health. Am J Perinatol. 2016;33(4):329–338. [PubMed: 26479171]
5. Jim B, Karumanchi SA. Preeclampsia: Pathogenesis, Prevention, and Long-Term Complications. Semin Nephrol. 2017;37(4):386–397. [PubMed: 28711078]
6. Demers S, Boutin A, Dembickaja R, Campanero M, Nicolaides K. Factors Associated with Placental Vascularization Measured by 3D Power Doppler Ultrasonographic Sphere Biopsy between 11 and 14 Weeks of Gestation. Am J Perinatol. 2018;35(10):964–971. [PubMed: 29458215]
7. Silverman RH, Urs R, Wapner RJ, Bearelly S. Plane-Wave Ultrasound Doppler of the Eye in Preeclampsia. Transl Vis Sci Technol. 2020;9(10):14.
8. Hypertension in pregnancy. Report of the American College of Obstetricians and Gynecologists' Task Force on Hypertension in Pregnancy. Obstet Gynecol. 2013;122(5):1122–1131. [PubMed: 24150027]
9. Spaide RF, Fujimoto JG, Waheed NK, Sadda SR, Staurenghi G. Optical coherence tomography angiography. Prog Retin Eye Res. 2018;64:1–55. [PubMed: 29229445]
10. Schindelin J, Arganda-Carreras I, Frise E, et al. Fiji: an open-source platform for biological-image analysis. Nat Methods. 2012;9(7):676–682. [PubMed: 22743772]
11. Li CH, Tam PKS. An iterative algorithm for minimum cross entropy thresholding. Pattern Recognition Letters. 1998;19(8):771–776.
12. Otsu N A Threshold Selection Method from Gray-Level Histograms. IEEE Transactions on Systems, Man, and Cybernetics. 1979;9(1):62–66.
13. Urs R, Ketterling JA, Yu ACH, Lloyd HO, Yiu BYS, Silverman RH. Ultrasound Imaging and Measurement of Choroidal Blood Flow. Translational vision science & technology. 2018;7(5):5–5.
14. Riskin-Mashiah S, Belfort MA, Saade GR, Herd JA. Transcranial doppler measurement of cerebral velocity indices as a predictor of preeclampsia. Am J Obstet Gynecol. 2002;187(6):1667–1672. [PubMed: 12501081]
15. Hata T, Hata K, Moritake K. Maternal ophthalmic artery Doppler velocimetry in normotensive pregnancies and pregnancies complicated by hypertensive disorders. Am J Obstet Gynecol. 1997;177(1):174–178. [PubMed: 9240603]
16. Hata T, Senoh D, Hata K, Kitao M. Ophthalmic artery velocimetry in preeclampsia. Gynecol Obstet Invest. 1995;40(1):32–35. [PubMed: 7557640]
17. Diniz AL, Moron AF, dos Santos MC, Sass N, Pires CR, Debs CL. Ophthalmic artery Doppler as a measure of severe pre-eclampsia. Int J Gynaecol Obstet. 2008;100(3):216–220. [PubMed: 17963761]
18. Sato T, Sugawara J, Aizawa N, et al. Longitudinal changes of ocular blood flow using laser speckle flowgraphy during normal pregnancy. PLoS One. 2017;12(3):e0173127. [PubMed: 28257508]
19. Alves Borges JH, Goes DA, de Araújo LB, Dos Santos MC, Debs Diniz AL. Prospective study of the hemodynamic behavior of ophthalmic arteries in postpartum preeclamptic women: A doppler evaluation. Hypertens Pregnancy. 2016;35(1):100–111. [PubMed: 26852911]

20. Onwudiegwu C, Adekanmi A, Olusanya B, et al. Case-control study on ocular changes and ophthalmic Doppler velocimetric indices among preeclamptic and normotensive pregnant women in Ibadan, Nigeria. BMJ Open Ophthalmol. 2020;5(1):e000550.
21. Barbosa AS, Pereira AK, Reis ZS, Lage EM, Leite HV, Cabral AC. Ophthalmic artery-resistive index and evidence of overperfusion-related encephalopathy in severe preeclampsia. Hypertension. 2010;55(1):189–193. [PubMed: 19948984]
22. Kane SC, Brennecke SP, da Silva Costa F. Ophthalmic artery Doppler analysis: a window into the cerebrovasculature of women with pre-eclampsia. Ultrasound Obstet Gynecol. 2017;49(1):15–21. [PubMed: 27485824]
23. Urfalıoglu S, Bakacak M, Özdemir G, Güler M, Beyoglu A, Arslan G. Posterior ocular blood flow in preeclamptic patients evaluated with optical coherence tomography angiography. Pregnancy Hypertens. 2019;17:203–208. [PubMed: 31487642]
24. Huppertz B Placental origins of preeclampsia: challenging the current hypothesis. Hypertension. 2008;51(4):970–975. [PubMed: 18259009]
25. Evcimen Y, Onur IU, Cengiz H, Yigit FU. Optical Coherence Tomography Findings in Pre-Eclampsia: A Preliminary Receiver Operating Characteristic Analysis on Choroidal Thickness for Disease Severity. Curr Eye Res. 2019;44(8):916–920. [PubMed: 30983421]
26. Sharudin SN, Saaid R, Samsudin A, Mohamad NF. Subfoveal Choroidal Thickness in Pre-eclampsia. Optom Vis Sci. 2020;97(2):81–85. [PubMed: 32011579]
27. Stern-Ascher CN, North VS, Garg A, Ananth CV, Wapner RJ, Bearelly S. Subfoveal Choroidal Thickness and Associated Changes of Angiogenic Factors in Women with Severe Preeclampsia. Am J Perinatol. 2021;38(5):482–489. [PubMed: 31683325]
28. Lupton SJ, Chiu CL, Hodgson LA, et al. Changes in retinal microvascular caliber precede the clinical onset of preeclampsia. Hypertension. 2013;62(5):899–904. [PubMed: 24019405]
29. Soma-Pillay P, Pillay R, Wong TY, Makin JD, Pattinson RC. The effect of pre-eclampsia on retinal microvascular caliber at delivery and post-partum. Obstet Med. 2018;11(3):116–120. [PubMed: 30214476]
30. Ciloglu E, Okcu NT, Dogan N. Optical coherence tomography angiography findings in preeclampsia. Eye (Lond). 2019;33(12):1946–1951. [PubMed: 31316159]

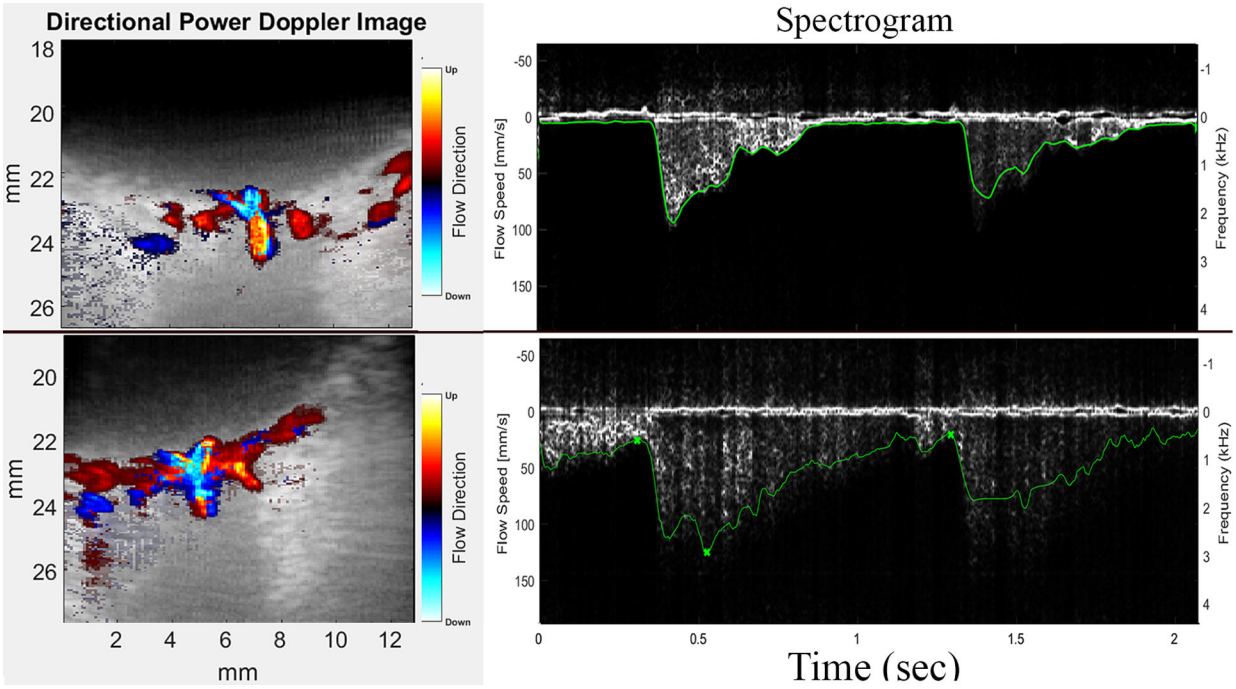

Figure 1:

Representative PWU color-flow images and spectrograms from a control (top) and an sPE subject (below). Note comparatively high end-diastolic flow velocity corresponding to reduced resistance in sPE.

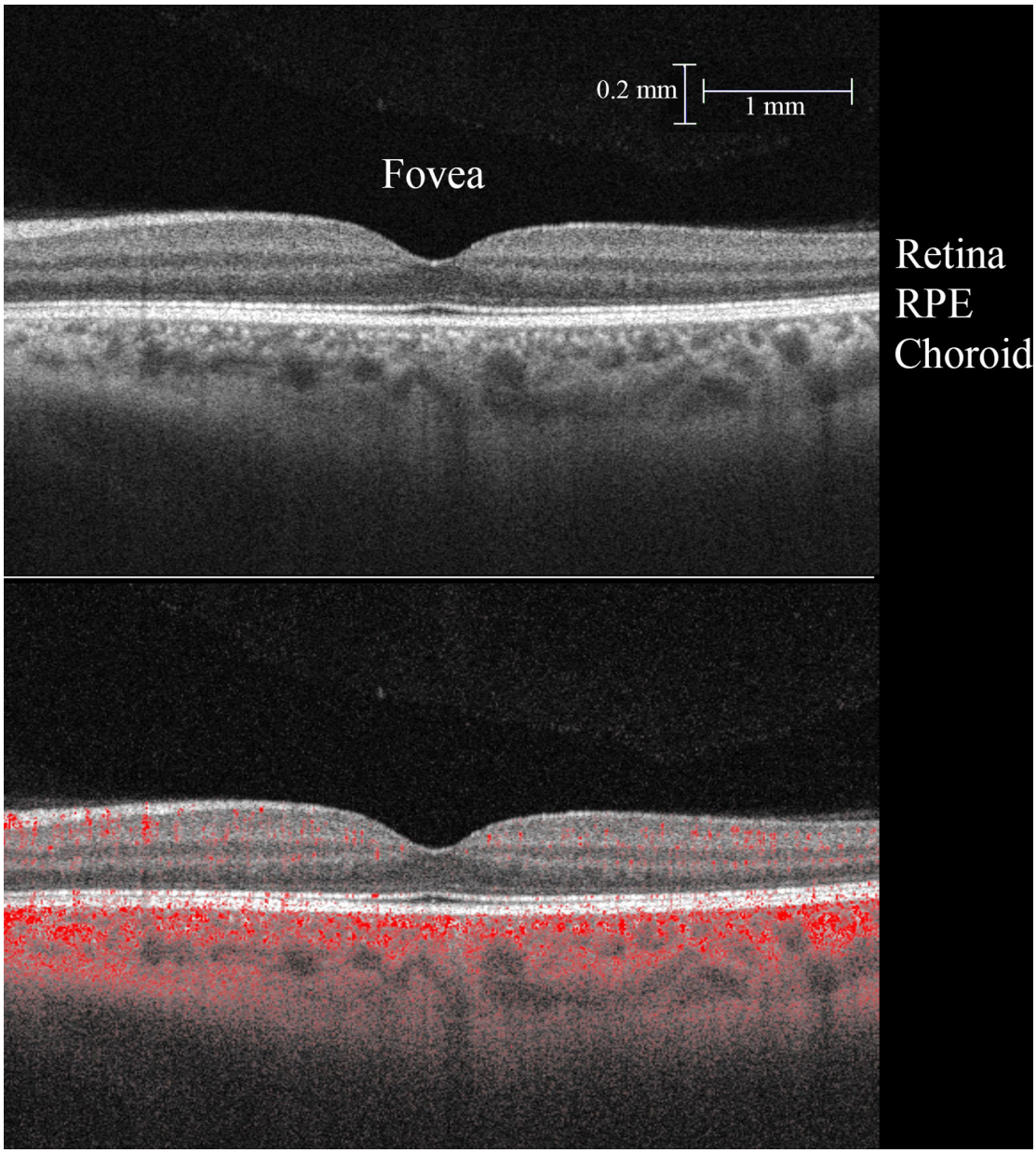

Figure 2:
Top: Representative perifoveal OCT B-scan. Below: Areas of signal decorrelation representing flow are superimposed in red over the grey scale B-scan. (RPE, retinal pigment epithelium)

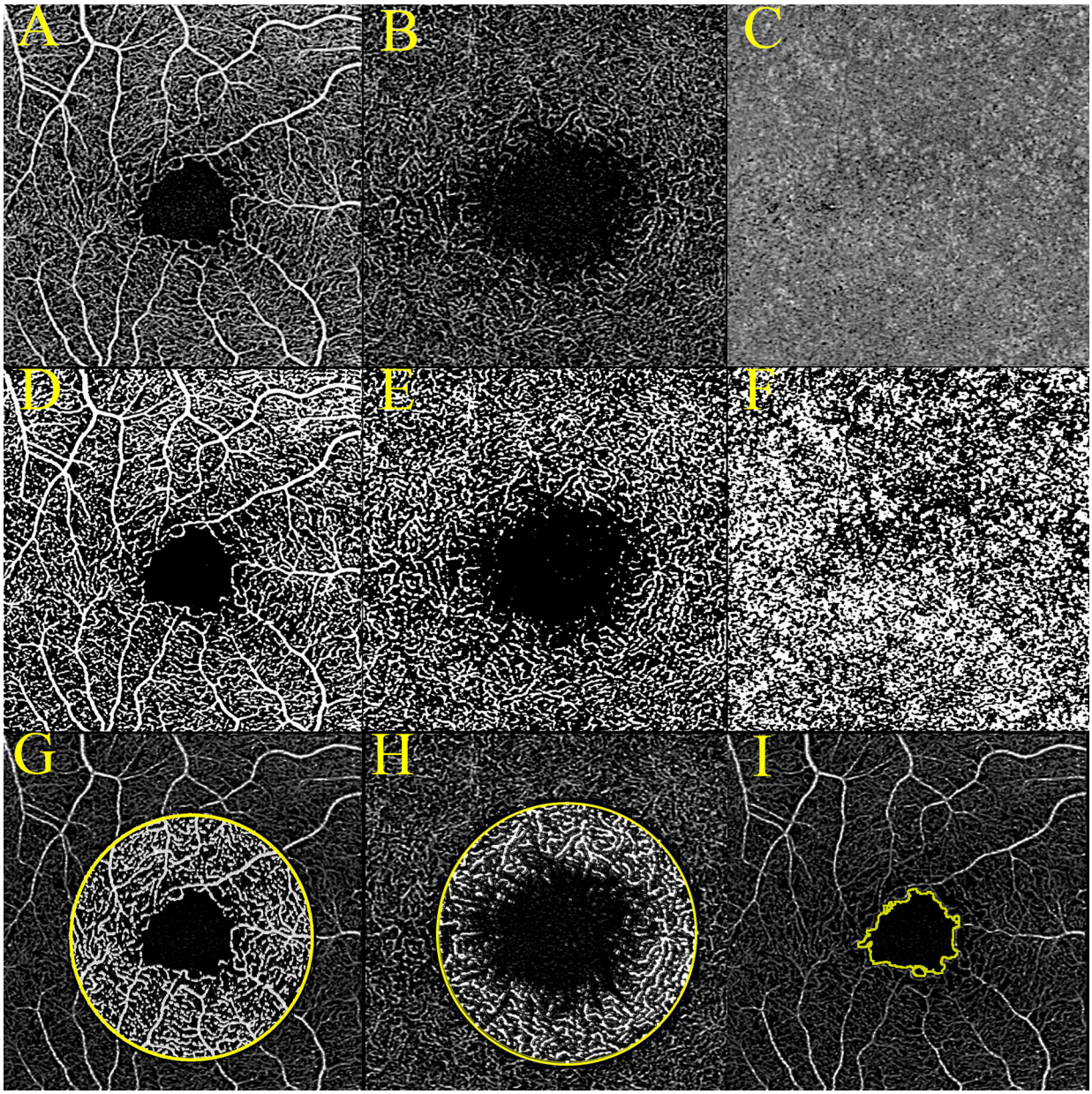

Figure 3:
OCTA images of perifoveal (A) superficial retina (B) deep retina and (C) choriocapillaris. Below (D to F) are corresponding thresholded binary images used for determination of VD. The Bottom row shows the 2-mm diameter perifoveal zone from which flow area is determined is illustrated in superficial (G) and deep (H) retina. (I) shows detection of the FAZ boundary.

Table 1.

ANOVA of systemic blood pressure (mmHg) and pulse rate in post-partum controls, mild PE (mPE), severe PE (sPE) and gestational or chronic hypertension (HTN).

Diagnosis	N	Systolic	Diastolic	MAP	PP	BPM
Control	11	114.6±13.8	73.7±9.4	87.3±10.6	40.9±6.4	71.5±7.1
mPE	5	129.4±10.4	79.4±7.2	96.1±7.5	50.0±8.0	75.8±.15.8
sPE	17	132.4±12.7*	82.7±7.5*	99.3±8.7*	49.6±8.4*	78.7±15.5
HTN	7	124.0±11.9	79.1±9.9	94.1±10.2	44.9±6.5	75.1±8.8
p		<.001	<.001	<.001	<.001	.097

MAP=mean arterial pressure, PP=pulse pressure, BPM=beats/minute. Significance of each group with respect to controls was assessed with post-hoc Dunnett's test:

* indicates p≤.05.

Table 2.

Correlation coefficients between systemic blood pressure and Doppler flow parameters by vessel.

Vessel	Parameter	Systolic	Diastolic	MAP	PP
	PSV	.008	−.014	−.0005	.030
	EDV	.003	.138	.081	−.144
Choroid	MV	.039	.014	−.010	−.084
	PI	−.068	−.092	−.022	.218
	RI	.027	−.134	−.065	.193
	PSV	.169	.006	.081	.288
	EDV	.236	.083	.157	.321*
CRA	MV	.157	.026	.087	.245
	PI	−.148	−.203	−.186	−.036
	RI	−.134	−.169	−.159	−.049
	PSV	−.030	−.009	−.019	.039
	EDV	−.020	−.201	−.129	.083
CRV	MV	.003	−.026	−.014	.033
	PI	−.045	−.185	−.130	.123
	RI	−.020	−.201	−.129	.182
	PSV	.052	.114	.090	−.033
	EDV	.188	.242	.227	.064
SPCA	MV	.104	.160	.140	.006
	PI	−.197	−.231	−.225	−.091
	RI	−.208	−.265	−.249	−.073

MAP=mean arterial pressure. PP=pulse pressure.

* indicates $p<.05$

Table 3.

Flow velocities (mm/sec) and resistance indices by group. Significance (p) is from GLM repeated measures analysis. Significance with respect to controls was assessed with post-hoc Dunnett's test:

Diagnosis	Vessel	N eyes	Peak Systolic	End Diastolic	Mean	RI	PI
Control	Choroid	22	9.50±3.06	4.27±1.19	6.17±1.66	.512±.140	.815±.340
mPE		10	9.40±2.09	4.23±1.25	5.91±1.46	.533±.150	.899±.359
sPE		34	8.98±2.00	4.93±1.07	6.54±1.26	.426±.122 *	.604±.229 *
HTN		14	10.83±2.73	4.45±1.35	6.72±1.51	.579±.078	.948±.200
p			.278	.231	.585	.<001	<.001
Control	CRA	22	81.57±24.59	11.00±7.54	31.95±11.61	.858±.088	2.41±.804
mPE		9	92.12±30.95	15.82±9.33	43.53±17.63	.825±.073	1.83±.408
sPE		34	81.62±22.79	13.03±6.58	37.13±12.10	.831±.076	1.98±.636
HTN		13	78.04±22.95	8.06±3.49	32.76±12.11	.884±.044	2.24±.486
p			.668	.194	.306	.258	.182
Control	CRV	14	33.87±13.06	16.45±7.12	24.21±9.53	.506±.137	.742±.302
mPE		8	37.78±11.31	20.34±6.07	28.11±7.99	.452±.109	.616±.188
sPE		25	31.19±12.14	19.77±8.26	24.89±9.87	.366±.139	.483±.215
HTN		11	29.84±11.84	16.55±7.60	23.03±9.77	.443±.129	.592±.221
p			.184	.675	.479	.147	.122
Control	SPCA	21	80.08±42.44	18.70±19.01	41.57±28.57	.789±.102	1.70±.530
mPE		10	91.44±28.78	21.89±14.95	45.75±21.85	.772±.079	1.66±.385
sPE		34	90.67±34.88	22.23±13.67	47.15±22.07	.758±.102	1.57±.481
HTN		14	79.85±29.76	14.24±6.80	39.92±17.43	.812±.052	1.71±.344
p			.816	.477	.825	.495	.771

* indicates p<.05

Table 4.

Correlation coefficients between ultrasound Doppler parameters and OCTA vascular density.

	Region	Perifoveal			Peripapillary
Vessel	**Parameter**	**Superficial**	**Deep**	**Chorio-capillaris**	**Superficial**
Choroid	PSV	.122	.030	−.019	.085
	EDV	−.160	.057	.142	−.190
	MV	−.056	−.033	.006	−.051
	PI	.258*	.019	−.140	.200
	RI	.255*	.022	−.164	.212
CRA	PSV	.164	.055	.296**	.213
	EDV	.015	.057	.163	−.113
	MV	.126	.030	.266*	.037
	PI	.059	.063	−.062	.283*
	RI	.149	.015	.026	.301**
CRV	PSV	.002	.038	−.251	−.045
	EDV	.162	.087	−.247	.119
	MV	.071	.045	−.267*	.046
	PI	.245	.052	−.026	.267*
	RI	.283*	.063	−.036	.236
SPCA	PSV	.047	−.096	.223*	.121
	EDV	−.035	.036	.235*	−.165
	MV	−.005	−.072	.210	.022
	PI	.118	−.064	−.082	.337**
	RI	.055	−.162	−.159	.380**

* indicates p≤.05,

** indicates p≤01.

Table 5.

Correlation coefficients between ultrasound Doppler parameters and OCTA flow area.

	Region		Perifoveal	
Vessel	**Parameter**	**Superficial**	**Deep**	**Chorio-capillaris**
Choroid	PSV	.142	−.100	−.169
	EDV	.033	.102	.020
	MV	.207	.018	−.168
	PI	.057	−.179	−.130
	RI	.135	−.143	−.180
CRA	PSV	−.157	−.173	.246*
	EDV	−.107	−.105	.225*
	MV	−.186	−.070	.300*
	PI	.098	−.139	−.151
	RI	.019	−.029	−.071
CRV	PSV	.113	.271*	−.040
	EDV	.126	.120	−.079
	MV	.101	.212	−.063
	PI	.014	−.211	−.080
	RI	.041	−.179	−.084
SPCA	PSV	−.096	−.129	.290**
	EDV	−.117	−.111	.293**
	MV	−.130	−.141	.270*
	PI	.133	−.035	−.105
	RI	.107	−.025	−.197

* indicates p≤05,

** indicates p≤01.